www.czasopisma.pan.pl PAN POLSKA AKADEMIA NAUK www.journals.pan.pl

Arch. Min. Sci. **68** (2023), 3, 375-392

Electronic version (in color) of this paper is available: http://mining.archives.pl

DOI: https://doi.org/10.24425/ams.2023.146857

KRZYSZTOF TAJDUŚ[1*], ANTON SROKA[2], MATEUSZ DUDEK[2], RAFAŁ MISA[2], STEFAN HAGER[3], JANUSZ RUSEK[1]

EFFECT OF THE ENTIRE COAL BASIN FLOODING ON THE LAND SURFACE DEFORMATION

This paper presents one of the environmental problems occurring during underground mine closures: according to the underground coal mine closure programme in Germany, the behaviour of the land surface caused by flooding of the entire planned mining area – the Ruhr District – had to be addressed. It was highlighted that water drainage would need to be continuous; otherwise, water levels would rise again in the mining areas, resulting in flooding of currently highly urbanised zones. Based on the variant analysis, it was concluded that the expected uniform ground movements caused by the planned rise in the mining water levels (comprising a part of two concepts – flooding up to the level of –500 m a.s.l. and −600 m a.s.l.), in the RAG Aktiengesellschaft mines, will not result in new mining damage to traditional buildings. The analysis included calculations of the maximum land surface uplift and the most unfavourable deformation factor values on the land surface, important from the point of view of buildings and structures: tilt T, compressive strain ε^{-} and tensile strain ε^{+}. The impact of flooding on potential, discontinuous land surface deformation was also analysed.

Keywords: Uplifts; land surface deformation; underground mining excavation flooding; mining damage; environmental problems; Ruhr District; Python

1. Introduction

Energy policy in Europe has radically changed in recent years, characterised by the move away from energy based on fossil fuel deposits, which contributed to significant technological

[1] AGH UNIVERSITY OF KRAKOW, AL. A. MICKIEWICZA 30, 30-059 KRAKÓW, POLAND
[2] STRATA MECHANICS RESEARCH INSTITUTES OF POLISH ACADEMY OF SCIENCE, 27 REYMONTA STR., 30-059 KRAKÓW, POLAND
[3] RAG AKTIENGESELLSCHAFT, ESSEN, GERMANY
* Corresponding author: krzytajdus@gmail.com

progress during the industrialisation era towards renewable energy. The reasons behind the current energy policy include dwindling deposits of energy resources, increasing costs for excavation, limits on CO_2 emissions, the impact of pollution on climate change and decreasing social approval for mining. The energy policy of the EU has resulted in the closures of underground coal mines, triggered by their unprofitability. The last coal mine in Germany, BW Prosper-Haniel, was closed in December 2018, and five mines in Poland were closed or scheduled for closure between 2015 and 2019 (KWK "Boże Dary", KWK "Brzeszcze Wschód", KWK "Mysłowice", KWK "Wieczorek I", KWK "Wieczorek II"). Currently, the closure plan for Polish coal mines foresees the closure of the last mine by 2049. In Czechia, closures of the mines owned by the OKD company, Lazy Mine and Darkov Mine, are currently underway, and all the company's mines are scheduled for closure by 2023.

However, the closure of an underground mine which has operated for many years is not easy, and many people are unaware of the related difficulties, costs and potential hazards [1,2]. In the vast majority of cases, the method of choice for mine closure is flooding because of the costs involved. This process means that once the preparations are complete, the mine switches off its systems pumping out mining water and reaching mine headings, and flooding takes place spontaneously [3-6]. Because of the increasing numbers of mine closures in Europe, a wide array of studies on the environmental impact of this process [7], identifying the risk of specific hazards occurring [2,8-10] and on mitigation of such hazards [11-14] has been undertaken in recent years.

It turns out that the hazards are considerably significant. Studies conducted in recent years indicate that when a mine is closed, methane pressure and concentration increase in the isolated post-mining voids, enabling further gas migration to the overburden or to directly connected mining headings [9,15]. Mining water contaminated with harmful elements may also penetrate ground waters [16-20]. In her work, Wysocka described the problem of radon emissions following underground coal mine closures and the harmful impact of such emissions on residents [21]. Mine closure by flooding also results in additional significant changes to the stress and deformation of the rock mass, manifesting on the surface as continuous [6,22,23] and discontinuous [24] deformations, and may also be observed as mining damage [4,23,25].

This paper aims to familiarise the reader with one of the significant environmental problems occurring during underground mine closures, namely land surface deformation, using the German Ruhr District as an example.

2. Land surface deformation resulting from mine closures by flooding

As was mentioned in the introduction, underground mine closure by flooding results in stress and deformation changes in the surrounding rock mass. These changes cause land surface deformations, the inverse of those related to underground mining operations: i.e. land surface uplift is observed. The first work on the possibility of forecasting this phenomenon was made by Pöttgens in 1985 [26]. He concluded that the rock mass, disrupted by underground mining, is characterised by increased porosity and permeability in the caved area compared to intact rock mass. The subsequent increase of mining water level during intentional flooding of the mine results in a pressure increase and expansion in the loose (caved) area as a consequence of increased normal stress values. The rock layers situated above the collapsed area experience an upward force known as buoyancy, which results in uplifts that can be seen on the land surface. A similar hypothesis on the genesis of this land surface uplift was presented by Fenk [27], who suggested that rising mining water levels lead to elastic expansion of the heavily cracked rock layers located in the roofs of the previously mined seams, resulting in additional uplift. An analysis of the available measurements of continuous displacements in the land surface may conclude that such a deformation does not threaten small buildings and non-linear structures. According to Pöttgens [26], the maximum land surface uplift may reach approx. 2% to 5% of the previous subsidence within the area in question, under the assumption that mining water reaches the surface level. This means that the uplift will be the most profound in areas with a history of the most intense excavations of multiple seams.

This situation is represented well by the example of the Königsborn mine in Germany. This mine was slated for closure due to its lack of profitability and energy policy. Water drainage from the mine stopped in mid-1996, which caused the mining water levels to rise (Fig. 1). Starting from this year, land surface uplift was observed as a consequence. Fig. 1 presents a graph with mining water level increase curves plotted as a function of time, with land surface uplift values recorded for three example measurement points. These points are located in different areas of the mine, where mining activity of various intensities took place in the past. The highest uplift was obtained at point 441900158 (marked in green), while the lowest uplift was observed at point 4312900245 (marked in pink) in an area where no coal mining took place.

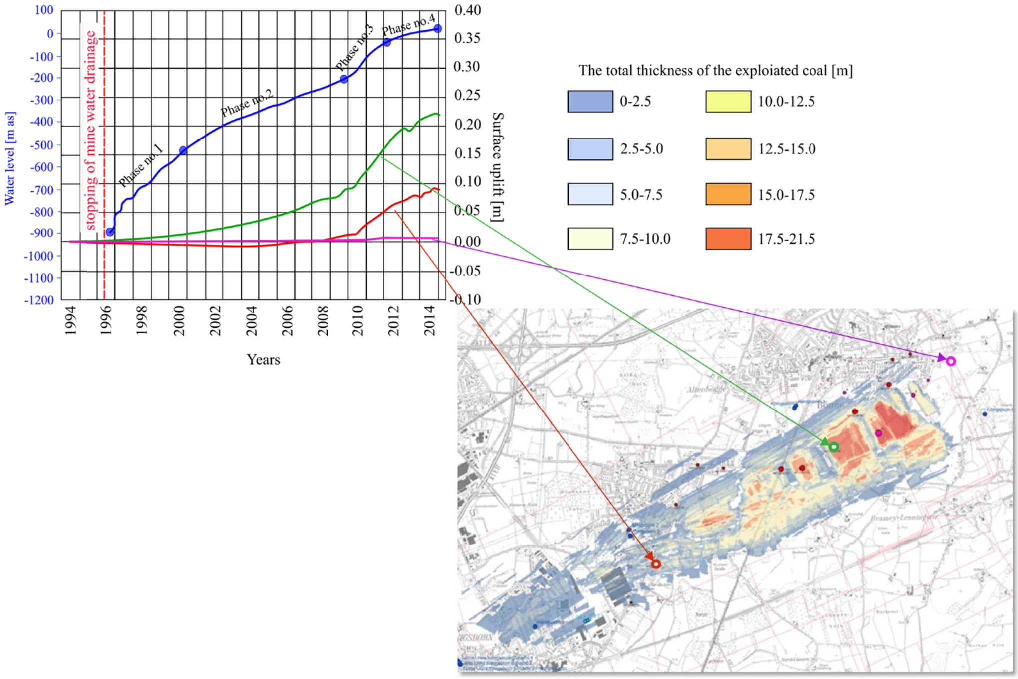

Fig. 1. Example land surface uplift during the flooding of the Königsborn mine
(own study based on RAG materials)

Measurements taken in the Warndt area in Saar, Germany, hint at the similar nature of such changes.

Fig. 2 presents the results of selected land surface uplift measurements, including the progressive increase of the mining water level during mine flooding. The left side of the figure presents the maps of excavations in the area, including the following marked depth ranges:

- excavations in the depth range of −180 to −400 m. a.s.l. during the period 1953-1978,
- excavations in the depth range of −400 to −600 m. a.s.l. during the period 1970-1983 and
- excavations in the depth range of −600 to −800 m. a.s.l. during the period 1974-2001.

As the data obtained by the RAG mining company shows, the C level was flooded between August 2005 and March 2008, the B level between March and September 2008 and the A level between September 2008 and January 2010. The mining water level inside the mine reached approx. −60 m underground during the subsequent stages of flooding.

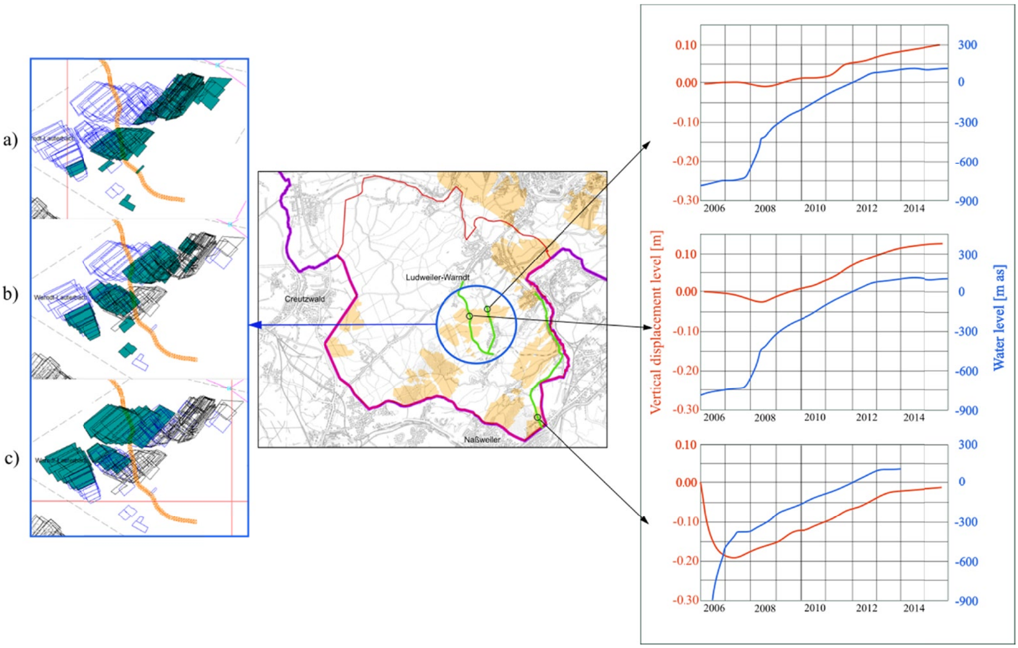

Fig. 2. Example land surface uplift during the flooding of the Warndt mining district (own study based on RAG materials)

As experience gained during the performed work shows, land uplift is strictly related to the intensity of past underground excavations in the given area. It also depends on the seam depth. According to the underground coal mine closure schedule in Germany, the land surface behaviour upon flooding of the entire planned mining area – the Ruhr District – had to be addressed. The answer to this issue is provided in this paper.

3. Review of methods for predicting surface deformation occurring in the liquidation of an underground mine by flooding

The problem related to forecasting changes in the state of displacement of the rock mass and land surface is quite recent from the point of view of the general problem of determining surface deformation during mining works. Therefore, there are not many models for predicting deformation in world literature.

There are two current types of approaches used in the field of modelling: analytical methods and numerical methods and modelling based on numerical methods. The first group includes solutions proposed by Pöttgens [26,28,29], Fenk [30,31] and Sroka [32-34]. In general, these methods are highly similar in terms of their theoretical bases in describing the causes of the uplift. The methods assume that land uplift is caused by increased pressure within the caved area, which is strictly related to the rising level of mining water. This process results in a volume increase in the caved area. The techniques used by Pöttgens and Fenk have significant drawbacks that prevent them from being effective in performing calculations for more complex scenarios. For example, Fenk's method refers to a single seam and does not consider the thickness of the broken rock zone above the mined-out coal seam. On the other hand, Pöttgens did not take into account, during deposit parameterisation, the lack of equilibrium in the volume balance in Geerstma's equation. Therefore, the calculated maximum surface subsidence can reach values greater than the compaction of the deposit itself in the case of a large gas reservoir.

Nowadays, Sroka's method is the most popular analytical solution. The authors presented in detail this solution, currently most often used in Germany and Poland

Sroka's method, used in the calculations of the uplift caused by rising mining water levels, is based on a cause-and-effect model, the structure of which corresponds to the Knothe method [35], used in calculations of land surface subsidence. The modification used here involves the inclusion of rock buoyancy caused by the rising mining water levels (Fig. 3).

According to Fig. 3, when we connect the cause (an increase in the volume of the caved area) to the transformation function, we can determine the amount of land surface uplift that occurs per unit. Sroka's method divides the caved area of every longwall panel into discrete, cuboid volume units [36]. The rock mass uplift is calculated for every such unit, and the obtained results are added together according to linear superposition. Such an approach allows buoyancy to be calculated for every surface point, with any exploitation's geometry, mining fields and seams.

To describe the distribution of land surface uplift when flooding a single unit within a caved area, we can use the following equation (1):

$$h(r,t) = \frac{k}{\pi} \cdot \frac{\Delta V(t)}{R_w^2} \cdot \exp\exp\left(-k\frac{r^2}{R_w^2}\right) \tag{1}$$

where

$$\Delta h(t) = d_m \cdot \Delta p(t) \cdot h \tag{2}$$

$$\Delta p(t) = \left[z_w(t) - Z_{Fl}\right] \cdot \gamma_w \tag{3}$$

k — the constant used in the Ruhrkohle method ($k = -\ln 0.01$),

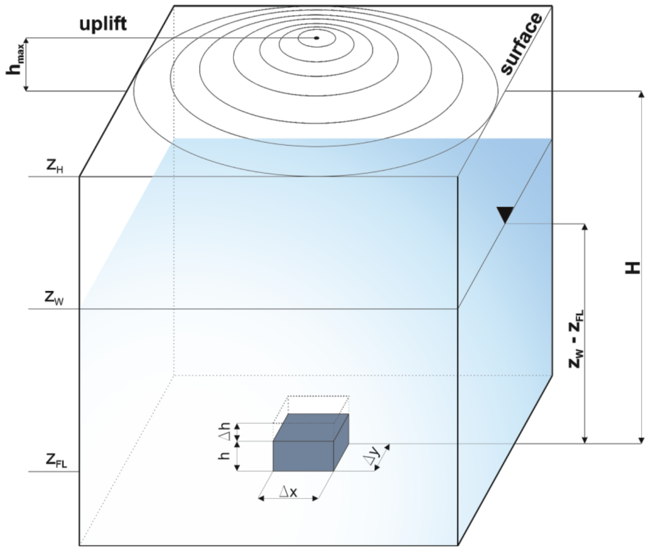

Fig. 3. Graphical explanation of the mathematical model of uplift caused by rising mining water levels [33]

d_m — the expansion coefficient, $d_m = \dfrac{\alpha}{E_s}$,
$\Delta p(t)$ — the pressure increase within the unit at time t,
$z_w(t)$ — the depth of the mining water level at time t,
Z_{Fl} — the seam depth,
r — the horizontal distance between the calculation point and the excavated area unit,
$\Delta V(t)$ — the unit volume of the caved area at time t, $\Delta V(t) = \Delta h(t) \cdot \Delta X^2$
ΔX — the length of the base side of a square caved area unit, $\Delta X = 0.1 R_w$
$\Delta h(t)$ — the height increase of a caved area unit at time t,
R_w — the radius of influence related to the rising mining water levels, $R_w = H \cdot \cot \gamma_h$,
H — depth of the fracture element,
γ_h — the angle of the main influence range during underground mine flooding,
h — the caved area unit height, $h = \lambda \cdot M$,
γ_w — the water weight,
λ — the relative caved area height,
M — the seam thickness,
Ms — the modulus of rigidity,
α — the Biot's coefficient.

The buoyancy coefficient should be determined for every unit of the caved area or every individual seam, according to equation (4).

$$a_h(t) = d_m \cdot \lambda \cdot \left[z_w(t) - Z_{Fl}\right] \cdot \delta_w \tag{4}$$

The values of parameters d_m and λ required for the calculation of the height increase of a caved area unit at a time (t) were determined and published by several authors based on in situ measurements using the parameter identification method. These include works by Pöttgens [26,28], Goerke-Mallet [37] and Sroka and Preuße [38-40] should be mentioned here. The results of these studies are summarised in TABLE 1.

TABLE 1

Summary of the characteristic values of d_m, λ and γ_w for selected coal mining areas in Germany

Mining area	d_m [m²/MN]	λ	$d_m \cdot \lambda$ [m²/MN]	γ_h [gon]
Südlimburger [26]	$0.350 \cdot 10^{-2}$	4	$1.40 \cdot 10^{-2}$	—
Ibbenbüren/ Westfeld [37]	$0.460 \cdot 10^{-2}$	3	$1.38 \cdot 10^{-2}$	—
Erkelenzer / Sophia Jacoba [38]	$0.265 \cdot 10^{-2}$	4	$1.06 \cdot 10^{-2}$	7.0-15.0 $\gamma_h = 12.0$
Ruhrrevier/ Königsborn [40]	$0.364 \cdot 10^{-2}$	3	$1.092 \cdot 10^{-2}$	12.0
Köningstein [41]	$0.222 \cdot 10^{-2}$	4	$0.890 \cdot 10^{-2}$	11.0-13.5

Particularly noteworthy are the values of the range angle of the main influences during mine flooding (γ_h), obtained from measurements and analyses for various mining regions, given in TABLE 1. These values differ significantly from the value of the angle of the range of main influences estimated for the exploitation (γ) and are contained in the relationship $\gamma = 0.08\gamma_h \div 0.10\gamma_h$. However, the range of γ_h is close to the value of the angle of the main influences related to the drainage basin.

Horizontal displacement of the land surface was calculated according to the hypothesis presented by Aviershin [42], which formulates a linear relationship between the horizontal displacement vector U and the tilt vector T:

$$U_i = B \cdot T_i, \quad i = 1{,}2 \tag{5}$$

where B is a proportionality factor.

The assumption in (6) implies a linear relationship between the horizontal strain tensor ε_{ij} and the vertical curvature tensor K_{ij}.

$$\varepsilon_{ij} = -B \cdot K_{ij}, \quad i = 1{,}2, \quad j = 1{,}2 \tag{6}$$

Equation (7) is used in the calculations of horizontal displacements of the land surface caused by rising mining water levels:

$$B_w = \frac{R_w}{\sqrt{2k}} = \frac{1}{3} R_w \tag{7}$$

The second approach is modelling based on numerical methods. Several procedures based on the finite element method (FEM) have been developed in Poland [4] and Germany [43]. The earliest solutions of this type [44,45] assumed that the pressure increase inside the caved area was caused by pressure applied to the immediate roof plane of the longwall panel. However, this solution rendered deformation predictions impossible, as it assumed a priori knowledge of the value of the changed pressure. This approach was modified in subsequent years by having it based on known geotechnical assumptions, with the bulk unit weight of the soil decreasing with the increasing water level within the soil (loosened rock) [4,46], according to the formula:

$$\gamma' = (1-n)(\rho_s - \rho_w)g \quad [\mathrm{kN/m^3}] \tag{8}$$

where

γ' — the volumetric weight of soil (rock)below the underground water level, [kN/m^3],
n — the porosity,
ρ_s — the soil (rock) density, [kg/m^3]
ρ_w — the water density, [kg/ m^3]
g — the gravity, [m/s^2].

This assumption allows predictive calculations for rock mass deformation to be performed for the flooded mines area, as was confirmed by measurements [4]. Unfortunately, despite its many advantages, numerical modelling has a limitation related to model complexity (the number of elements and nodes), which is a direct function of the size of the area. The models used in the past were limited to a single mine area (rock mass within a wall [47-51], a wall system [52-54] or a seam system [55-57]). Scientists have developed numerical models for entire mines in various instances [4,46,58-60]. However, due to the high number of elements and nodes involved, these calculations, including model calibration, were exceedingly arduous and time-consuming.

4. Land surface deformation prediction for flooding of mines in the Ruhr District (Prosper Province)

4.1. Description of the analysed mining area

The analysed area is extremely varied. It covers approx. 60 km in the E–W direction and approx. 35 km in the S–N direction; 2,100 km^2 in total. It is characterised by the extreme density of buildings and the presence of numerous industrial sites, refineries, channels and waterways, local airports, oil and gas pipelines and heritage and cultural sites (Fig. 4). This variety is a result of the presence of several cities with more than 300,000 residents in the area, such as Essen and Bochum, as well as cities with more than 100,000 residents, such as Mülheim an der Ruhr, Oberhausen, Bottrop, Gelsenkirchen, Recklinghausen and Herne, including the related (and equally extensive) public, road and railway infrastructure.

The covered area includes the following closed coal mines: Lohberg, Prosper-Haniel, Amalie, Zollverein, Carolinenglück, Fürst Leopold and Auguste Victoria.

These mines were the locations of mining activity, starting from the 18th century until 2018. Approximately 120,000 excavation fields were mined during this period, with various shapes, depths and levels of structural firmness, as well as different excavation rates and excavation systems used.

4.2. Description of the assumptions used in numerical analysis

The area analysed in this paper includes seven mines, where the excavation took place over several centuries, and covers 2,100 km^2, as well as depth down to 1,500 m a.s.l. The development of such a vast numerical model while following all development rules related to the size

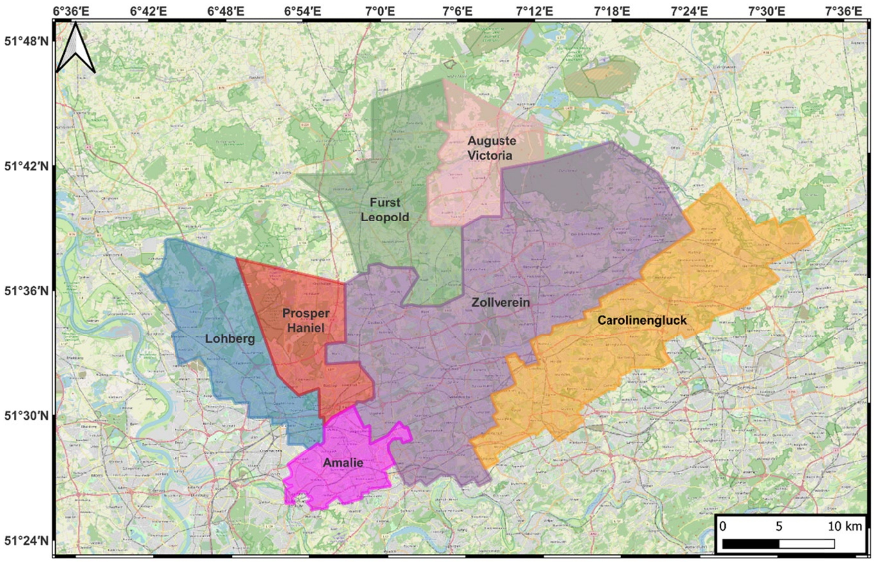

Fig. 4. Map of the analysed area, showing the areas of the closed coal mines

of the units, the distance to boundary conditions, etc., is virtually impossible using the current computational capacity. Thus, the authors used a hybrid method in the predictive calculations, integrating the analytical approach and a simplified numerical method. The model by Sroka [39] was selected as the analytical model. The numerical integration method was used to fit the model to the space over the outline of the flooded excavations within the studied mining area. This model offers several significant advantages over the other methods; for instance, it allows deformation calculations for a multi-seam mining operations to be performed according to the superposition method, thus ensuring high-quality results and excellent conformity with precise measurements. The validity of this approach has been confirmed for many German and Polish mines [34,40]. The numerical implementation of analytical relationships was possible only thanks to data related to values of geometric, mining and geomechanical parameters, which were obtained through long-term observations of more than 120,000 longwalls. The data was highly dispersed due to the method used for data archiving and the dedicated numerical tools used to extract it. A controlling programme written in Python was created to compress the data effectively, resulting in a cohesive set of input variables for further analysis. This programme was created with the future collectivisation of data for the development of a complex stochastic model in mind, intended to replace the emulation-based approach presented in this work, according to the authors. The selection of Python as a programming language was dictated by the fact that it has been widely used in Data Science in recent times and enables data acquisition in real-time. Finally, a simplified numerical model was created.

The model automatically divided all exploited areas into cuboid volume units with base side lengths ΔX equal to $\Delta X = \sqrt{H}$ and height h equal to the height of the caved area. The relevant values of geometric, mining and geomechanical parameters were assigned to such units (according to the parameters presented in Equation 1). The next stage involved numerical integration performed in Python. The results were saved in a separate data file in each case.

4.3. Results of calculations performed for the entire Ruhr District

The closure schedule for the RAG Aktiengesellschaft mines assumes that the mining water levels will rise up to −600 m a.s.l. throughout the entire area (Prosper Province). Analyses were made for two final water levels: the final level of −600 m a.s.l. and the level of −500 m a.s.l.

The previously described hybrid model provided the basis for estimating the predicted land surface displacements. An analysis of the data presented in TABLE 1 revealed that the most representative values of parameters were determined for the closed mining area of Königsborn. The following values for the model parameters were used in the calculations: $d_m = 0.364 \cdot 10^{-2}$ m^2/MN, $\lambda = 3.0$, and $\gamma_h = 12$ gons.

Information on the height of the caved area for individual mining fields was determined during a local interview performed at RAG Aktiengesellschaft. The calculations were performed for all seams, longwalls and other exploitation fields present.

The number of effective, performed mining goafs for the rise of the mining water level to the planned final level of −600 m a.s.l. was 12,275; in the second scenario (−500 m a.s.l.), the number of goafs was 17,520 (Fig. 7) in 22 seams.

Calculations were performed for the data prepared as described above. The predicted distributions of uplift in the analysed area are presented in Figs. 5 and 6 for the two levels −600 m a.s.l. and −500 m a.s.l.

These figures clearly show local concentrations of land surface uplift intensity. They are located in individual water provinces and are directly related to the intensive and concentrated extraction at some of the former coal mines, such as Lohberg and Auguste Victoria (Fig. 7).

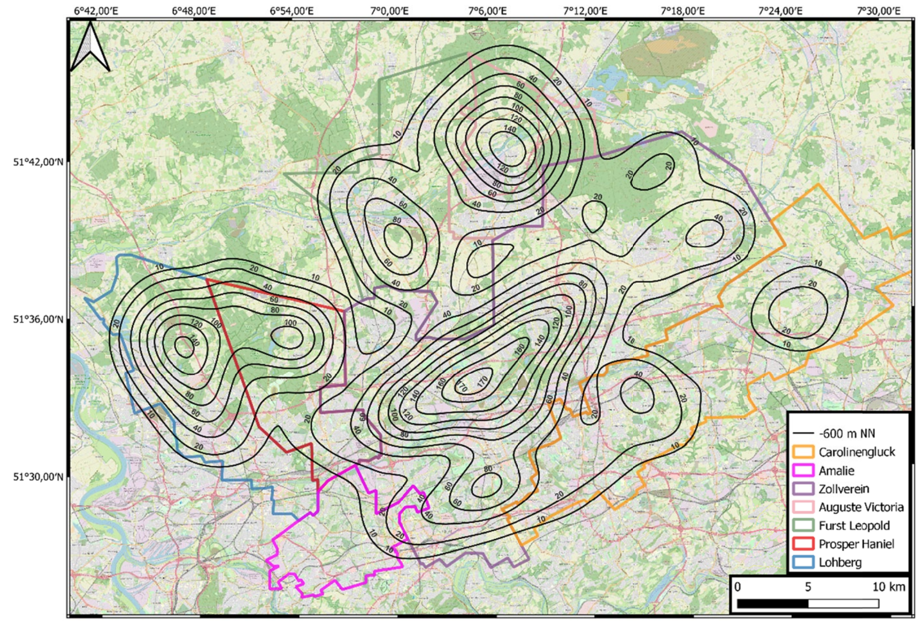

Fig. 5. The predicted distribution of uplift within the analysed area assumes a mining water level rise up to −600 m a.s.l.

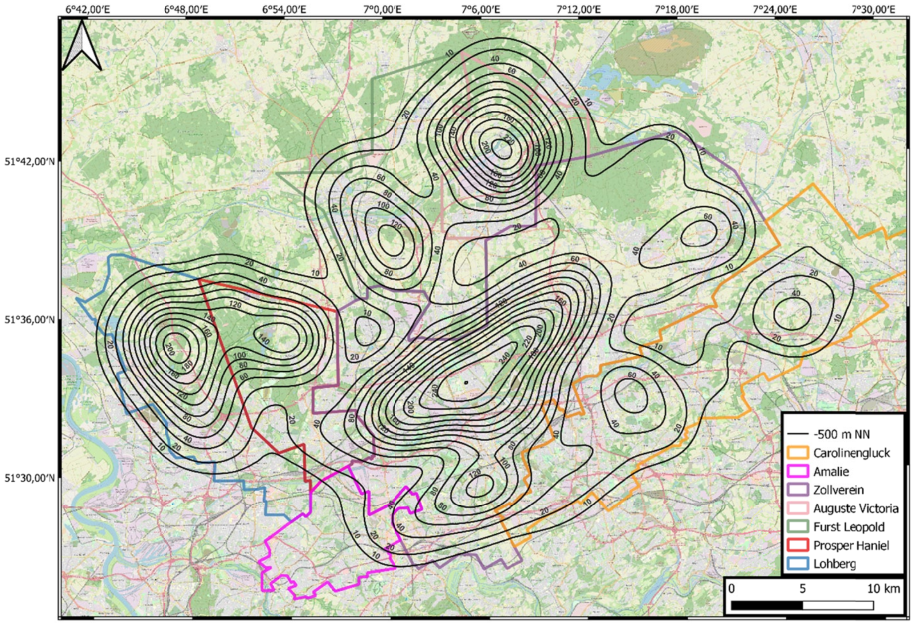

Fig. 6. The predicted distribution of uplift within the analysed area assuming mining water level rises up to −500 m a.s.l.

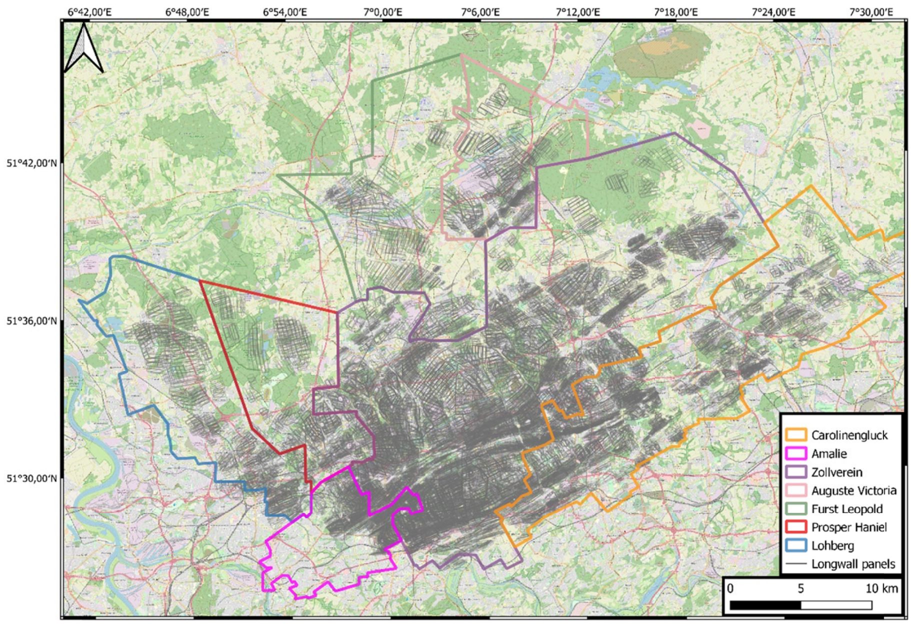

Fig. 7. A representation of the goafs taken included in the mine flooding schedule, up to the level of −500 m a.s.l. (Kartengrundlage: © Regionalverband Ruhr, CC-BY 4.0)

TABLE 2 provides a summary of the calculated extreme values for land surface uplift (h_u) and representative values (from the point of view of preventive measures used in construction) and land surface deformation indicators: tilt T, horizontal compressive (ε^-) and tensile (ε^+) strain [61,62]. According to the table, the Zollverein area had the highest values of calculated deformation indicators. The predicted value of land surface uplift was approx. 175 mm, assuming the mining water level rises up to −600 m a.s.l., and approx. 258 mm with the reference level of the mining water column fixed at the depth of −500 m a.s.l. It should be noted that the other predicted values of deformation indicators are insignificant and do not exceed 0.1 mm/m.

TABLE 2

Summary of predicted values of land surface deformation assuming mine flooding in two scenarios

Mining area	Maximum values of land deformation indicators							
	Flooding scenario up to the level of −600 m a.s.l.				Flooding scenario up to the level of −500 m a.s.l.			
	h_u [mm]	T [mm/m]	ε^- [mm/m]	ε^+ [mm/m]	h_u [mm]	T [mm/m]	ε^- [mm/m]	ε^+ [mm/m]
Lohberg	145	0.050	–0.030	0.046	213	0.087	–0.053	0.079
Prosper-Haniel	108	0.038	–0.023	0.034	159	0.065	–0.039	0.059
Zollverein	175	0.061	–0.037	0.055	258	0.106	–0.064	0.096
Carolinenglück	48	0.017	–0.010	0.015	71	0.029	–0.018	0.026
Fürst Leopold	87	0.030	–0.018	0.028	129	0.053	–0.032	0.048
Auguste-Victoria	153	0.053	–0.032	0.048	226	0.092	–0.056	0.084

Comparative calculations for two flooding scenarios for the mining areas led to a conclusion that the mining water level was 100 m above the level of −600 m a.s.l. – will result in an approx. 50% increase in the maximum land surface uplift. Despite this, the predictive calculations showed that the remaining values of deformation indicators will not result in a significantly increased risk of damage to buildings and structures. The ratio of the maximum land surface uplift for the mining water column level rising up to −500 m a.s.l. to the rise up to −600 m a.s.l. is approximately constant for all calculation points and equals 1.48. The increase of the maximum uplift level results from the significantly increased number of the analysed former mining areas and an increase in the number of mining panel exploitation.

5. Discussion

The results of these studies indicate that one of the considered flooding scenarios planned for mines owned by RAG Aktiengesellschaft will not result in an increased risk of damage to buildings and structures located within the areas of the former coal mines. This is due to the relatively low values of predicted deformation indicators, which reach several per cent of the deformation observed during mining operations. This applies in particular to the horizontal land deformation indicator, which is responsible for most of the mining damage within mine areas [63-65]. TABLE 3 contains absolute limit values for horizontal land surface deformation which, if exceeded, can lead to damage to buildings and structures, according to various authors.

TABLE 3

Limit values for horizontal land surface deformation, significant from the point of view of damage to buildings and structures

Author	Absolute limit value of horizontal deformation ε_{Gr} [mm/m]
Pöttgens [26]	0.25
Sroka & Grün (1993)	0.25
Schmidt-Schleicher [66]*	0.10
Staege & Pohl [67]	0.20
Kwiatek, et al. [65]	0.30

* The limit specified by Schmidt-Schleicher is characteristic for historical buildings.

The initially calculated maximum values of land surface deformation indicators are much lower than the absolute limit values accepted by the experts (TABLES 2 and 3). Thus, the increased risk of structural damage related to active mining operations may be excluded in the case of detached and terraced residential buildings.

The impact of flooding on the possible discontinuous land deformation is another problem which should be considered. Recent years saw the increased interest of the general public in this topic, caused by certain incidents, i.e. during the flooding of the Sophia-Jacoba coal mine [68], where water drainage was stopped in 1997. Activation of the Meinweg and Rurrand faults was observed between 1999 and 2004 as the mining water level rose. This activation led to a linear deformation with a total length of 9 km, resulting in damage to ca. 110 buildings and structures [69]. It should be noted that stress accumulation and displacements along the fault area very often take place during the initial multi-seam mining operations. The flooding stage, on the other hand, results in decreased stress, a lower angle of internal friction and decreased cohesion of the material filling the fault. Thus, it is an indirect cause of discontinuous activation of such faults and the damage line formation. According to in situ studies performed for almost 1,000 cases [70,71], the limit value of rock mass deformation potentially resulting in fault activation is 2.0 mm/m. These findings are related to the consequences of the mining water level rising almost to the surface level. In the analysed scenarios (−600 m and −500 m a.s.l.), the planned flooding will have a much smaller effect, and, probably, flooding will not result in a discontinuous deformation.

To the best knowledge of the authors, changes to the mine flooding scenario in the future are unlikely. This is related to the safety of underground reservoirs of tap water and thermal water. In the future, the tool developed during the study can be utilised to establish a database with a specific structure that prioritises the safety and transparency of reservoirs. To adapt the data archiving process to the criteria mentioned above, the use of the BlockChain methodology is considered at this stage. The results of the current analysis will provide the data required to create a machine learning-based model, particularly models based on Bayes conclusion formalism (Bayesian networks, dynamic Bayesian networks). Such a plan of studies implemented in practice should result in a representation of the analysed phenomenon. A properly calibrated representation model can additionally allow for the prediction of cases with sets of input parameters different from those used in learning, thus significantly expanding the applicability of the model. Additionally, because of the implementation of methodology based on the Bayes conclusion formalism, the model will be able to evolve as new data sets become available. This property enables such a model to be implemented within the framework of structural health monitoring and matches the concepts of sustainable development and Industry 4.0.

6. Conclusions

The number of mines closed in recent years is on the rise, and there has been an increase in social initiatives related to the elimination of CO_2 and CH_4 emissions and economic aspects. However, closures of underground mining excavations by flooding are an extremely costly and complex process in the long term. This results in numerous problems, both socioeconomic issues and threats to surface infrastructure. In this paper, the authors focus on calculations of predicted indicators of land surface deformation for the entire German mining area. The analysis led to the following conclusions:

1. It may be concluded that the expected uniform ground movements caused by the planned mining water level rise, as indicated in two proposals for the RAG Aktiengesellschaft, mines will not result in an increased risk of new mining damage to traditional buildings.
2. The deformation range during flooding is much greater than the related range for the mining operations, meaning that objects (linear objects, in particular) initially present outside the specified range of influence may fall within this range in the mine flooding scenario. Their magnitude, however, is small in the case of linear and special objects, and their technical condition should be monitored and their safety assessed periodically.
3. According to current experience and knowledge, discontinuous land surface displacements in the area of tectonic faults and the formation of discontinuous deformations should also not be expected.
4. In the case of a scenario change and the mining water level rising to the surface, the formation of a discontinuous linear deformation cannot be excluded in the area where large tectonic faults are present. This scenario should also include the possible occurrence of local, discontinuous surface deformations in areas where mining excavations are present at shallow levels.

To further conclude, when creating a plan for flooding an underground mine, it is crucial to consider that it is incredibly difficult to return the area to its original condition before the mines were built. The above was also noted by Szwedzicki [72] in concern to Australian mines. In addition, water drainage should be continued indefinitely because of the past mining activity and the resulting land surface subsidence, namely changes to the land surface shape. Otherwise, the risks of water reservoir levels in mining areas being restored and of flooding in heavily urbanised areas cannot be eliminated.

References

[1] D. Laurence, Classification of risk factors associated with mine closure. Miner. Resour. Eng. **10**, 3, 315-331 (2001). DOI: https://doi.org/10.1142/S0950609801000683

[2] S. Amirshenava , M. Osanloo, Mine closure risk management: An integration of 3D risk model and MCDM techniques. J. Clean. Prod. **184**, 389-401 (2018). DOI: https://doi.org/10.1016/j.jclepro.2018.01.186

[3] A. Krzemień, A. Suárez Sánchez, P. Riesgo Fernández, K. Zimmermann, F. González Coto, Towards sustainability in underground coal mine closure contexts: A methodology proposal for environmental risk management. J. Clean. Prod. **139**, 1044-1056 (2016). DOI: https://doi.org/10.1016/j.jclepro.2016.08.149

[4] M. Dudek, K. Tajduś, R. Misa, A. Sroka, Predicting of land surface uplift caused by the flooding of underground coal mines – A case study. Int. J. Rock Mech. Min. Sci. **132** (2020). DOI: https://doi.org/10.1016/j.ijrmms.2020.104377

[5] J.M. Reyes-Montes, B.L. Sainsbury, J.R. Andrews, R.P. Young, Application of cave-scale rock degradation models in the imaging of the seismogenic zone. CIM J. **7**, 2, 87-92 (2016). DOI: https://doi.org/10.15834/cimj.2016.9

[6] A. Vervoort, P.-Y. Declercq, Surface movement above old coal longwalls after mine closure. Int. J. Min. Sci. Technol. **27**, 3, 481-490 (2017).

[7] M. Caro Cuenca, A.J. Hooper, R.F. Hanssen, Surface deformation induced by water influx in the abandoned coal mines in Limburg, The Netherlands observed by satellite radar interferometry. J. Appl. Geophys. **88**, 1-11 (2013). DOI: https://doi.org/10.1016/j.jappgeo.2012.10.003

[8] K. Skubacz et al., Modelling of radon hazards in underground mine workings. Sci. Total Environ. **695**, 133853 (2019).

[9] A. Duda , A. Krzemień, Forecast of methane emission from closed underground coal mines exploited by longwall mining – A case study of Anna coal mine. J. Sustain. Min. **17**, 4, 184-194 (2018). DOI: https://doi.org/10.1016/j.jsm.2018.06.004

[10] A. Krzemień, A.S. Sanchez, P.R. Fernandez, K. Zimmermann, F.G. Coto, Towards sustainability in underground coal mine closure contexts: A methodology proposal for environmental risk management. J. Clean. Prod. **139**, 1044-1056 (2016).

[11] "Management of environmental risks during and after mine closure, Contract No. RFCR-CT-2015-00004," 2020.

[12] A.C. Sanchez, L.E. Silva-Sanchez, S.S. Neri, Guide for mine closure, no. June. 2014.

[13] P.M. Heikkinen et al., Mine Closure Handbook – Environmental Techniques for the Extractive Industries. 2008.

[14] C. Didier et al., Mine Closure and Post-Mining Management International State-of-the-Art International Commission on Mine Closure International Society for Rock Mechanics, no. November 2008, (2008). DOI: https://doi.org/10.13140/2.1.3267.8407

[15] E. Krause, Z. Pokryszka, Investigations on Methane Emission from Flooded Workings of Closed Coal Mines. J. Sustain. Min. **12**, 2, 40-45 (2013). DOI: https://doi.org/10.7424/jsm130206

[16] L. Jorge et al., Surface water monitoring in abandoned mercury mine sites in Asturias (Spain): Comparative Studies, 595-601 (2003).

[17] D. Johnston, H. Potter, C. Jones, S. Rolley, I. Watson, J. Pritchard, Abandoned mines and the water environment, no. SC030136/SR41\rSCHO0508BNZS-E-P. 2008.

[18] J. Bondaruk, E. Janson, M. Wysocka, S. Chałupnik, Identification of hazards for water environment in the Upper Silesian Coal Basin caused by the discharge of salt mine water containing particularly harmful substances and radionuclides. J. Sustain. Min. **14**, 4, 179-187 (2015). DOI: https://doi.org/10.1016/j.jsm.2016.01.001

[19] S. Corbel, J. Kaiser, S. Vicentin, Coal Mine Flooding in the Lorraine-Saar Basin: Experience from the French Mines. IMWA 2017 – Mine Water Circ. Econ. **1**, 161-166 (2017). [Online]. Available: file:///N:/Literatur/Literatur/IMWA Proceedings/imwa_2017/IMWA2017_Corbel_161.pdf.

[20] J. Zeman, M. Černík, I. Šupíková, Dynamic model of long term geochemical evolution of mine water after mine closure and flooding. no. February 2016, pp. 828-836, (2009).

[21] M. Wysocka, Radon in the investigations of geo-hazards in Polish collieries. Geofluids, **10**, 4, 564-570 (2010). DOI: https://doi.org/10.1111/j.1468-8123.2010.00306.x

[22] S. Samsonov, N. D'Oreye, B. Smets, Ground deformation associated with post-mining activity at the French-German border revealed by novel InSAR time series method. Int. J. Appl. Earth Obs. Geoinf. **23**, 142-154 (2013). DOI: https://doi.org/10.1016/j.jag.2012.12.008

[23] A. Vervoort , P.-Y. Declercq, Upward surface movement above deep coal mines after closure and flooding of underground workings. Int. J. Min. Sci. Technol. **28**, 1, 53-59 (2018). DOI: https://doi.org/10.1016/j.ijmst.2017.11.008

[24] D.P. Sainsbury, B.L. Sainsbury, L.J. Lorig, Investigation of caving induced subsidence at the abandoned Grace Mine. Trans. Institutions Min. Metall. Sect. A Min. Technol. **119**, 3, 151-161 (2010).
DOI: https://doi.org/10.1179/174328610X12820409992336

[25] K. Tajduś, A. Sroka, R. Misa, M. Dudek, Przykłady zagrożeń powierzchni terenu deformacjami nieciągłymi typu powierzchniowego ujawniające się nad zlikwidowanymi podziemnymi wyrobiskami górniczymi. Pr. Inst. Mech. Górotworu PAN **19**, 3, 3-10 (2017).

[26] J.J.E. Pöttgens, Bodenhebung durch ansteigendes Grubenwasser," in 6. Internationaler Kongress für Markscheidewesen, pp. 928-938, (1985).

[27] J. Fenk, Hebungen der tagesoberflache uber stillgelegten steinkohlenbergwerken im Zwickau-Oelsnitzer Revier (diskussionsbeitrag) (DISKUSSIONSBEITRAG). Freib. Forschungshefte. R. A **847**, 208-234 (1998).

[28] J.J.E. Pöttgens, Bodenhebung und Grundwasseranstieg aus geotechnischer und markscheiderisch-geodätischer Sicht im Aachen-Limburger Kohlenrevier. Freib. Forschungshefte, Bergbau und Geotech. **847**, 193-207 (1998).

[29] R.F. Bekendam, J.J.E. Pöttgens, Ground movements over the coal mines of southern Limburg, The Netherlands, and their relation to rising mine waters, in 5tfh international symposium on land subsidence, pp. 3-12, (1995).

[30] J. Fenk, Eine analytische Lösung zur Berechnung von Hebungen der Tagesoberfläche bei Flutung unterirdischer Bergwerksanlagen. Markscheidewesen **107**, 4220-4422 (2000).

[31] J. Fenk, D. Tzscharschuch, Zur Berechnung flutungsbedingter Hebungen der Tagesoberfläche. Markscheidewesen **114**, 2, 60-64 (2007).

[32] A. Sroka, J. Fenk, Studie zu Auswirkungen des Grubenwasseranstiegs auf Bewegungen der Tagesoberfläche in stillgelegten Bergbaubereichen des Saarlandes, (2003).

[33] A. Sroka, Ein Beitrag zur Vorausberechnung der durch den Grubenwasseranstieg bedingten Hebungen, in 5. Altbergbau-Kolloquium, pp. 453-462, (2005).

[34] A. Sroka, A. Preuβe, M. Holzheim, Auswirkung des Grubenwasseranstiegs auf die Tagesoberfläche – Stand der Forschung, in 8. Aachener Altlasten- und Bergschadenkundliches Kolloquium, pp. 57-68, (2006).

[35] S. Knothe, Effect of time on formation of basin subsidence. Arch. Min. Steel Ind. **1**, 1, 1-7 (1953).

[36] A. Sroka, Contribution to the Prediction of Ground Surface Movements Caused by a Rising Water Level in a Flooded Mine. In Proceedings International Mining forum, pp. 57-68 (2006).

[37] P. Goerke-Mallet, Untersuchungen zu raumbedeutsamen Entwicklungen im Steinkohlenrevier Ibbenbüren unter besonderer Berücksichtigung der Wechselwirkungen von Bergbau und Hydrogeologie. Rheinisch- Westfälischen Technischen Hochschule Aachen, (2000).

[38] A. Preuβe, A. Sroka, Projekt Risiken durch Grubenwasseranstieg. 3. Zwischenbericht, (2008).

[39] A. Sroka, A. Preuβe, Zur Prognose flutungsbedingter Hebungen. in 9. Altbergbau-Kolloquium, pp. 184-196, (2009).

[40] A. Preuβe, A. Sroka, Schlussbericht zum Forschungsvorhaben „Risiken durch Grubenwasseranstieg", Herne (2015).

[41] A. Graovski, A. Sroka, C. Wedekind, Untersuchungen zu Auswirkungen an der Tagesoberfläche nach Einleitung der Flutung am Beispiel des Sanierungsstandortes Königstein der Wismut GmbH. In 14. Geokinematischer Tag, pp. 60-74, (2013).

[42] S.G. Aviershin, Mining subsidence engineering (in Russian). Moscow, Russia: Handbook, Ugletiechizdat.

[43] J. Zhao, H. Konietzky, Numerical analysis and prediction of ground surface movement induced by coal mining and subsequent groundwater flooding. Int. J. Coal Geol. **229**, p. 103565, Sep. (2020).
DOI: https://doi.org/10.1016/j.coal.2020.103565

[44] W. Milczarek, Analiza zmian powierzchni górotworu po zakończonej eksploatacji górniczej w wybranym rejonie dawnego Wałbrzyskiego Zagłębia. Politechnika Wrocławska, (2011).

[45] M. Wesołowski, R. Mielimąka, M. Jendruś Rafałand Popczyk, Influence Analysis of Mine Flooding from the Environmental Standpoint: Surface Protection. Polish J. Environ. Stud. **27**, 2, 905-915 (2018).
DOI: https://doi.org/10.15244/pjoes/76114

[46] M. Dudek , K. Tajduś, FEM for prediction of surface deformations induced by flooding of steeply inclined mining seams. Geomech. Energy Environ., p. 100254, Apr. (2021).
DOI: https://doi.org/10.1016/j.gete.2021.100254

[47] K. Tajduś, Numerical simulation of underground mining exploitation influence upon terrain surface. Arch. Min. Sci. **58**, 3 (2013).

[48] K. Tajduś, A. Sroka, A. Tajduś, A. Preusse, Three dimensional modeling of a surface displacements as a result of an underground longwall panel extraction. Proceedings – 29th International Conference on Ground Control in Mining, ICGCM, pp. 105-110 (2010).

[49] S.R. Islavath, D. Deb, H. Kumar, Development of a roof-to-floor convergence index for longwall face using combined finite element modelling and statistical approach. Int. J. Rock Mech. Min. Sci. **127**, 104221, Mar. (2020). DOI: https://doi.org/10.1016/j.ijrmms.2020.104221

[50] R. Pan et al., A new model for the identification of subcritical surface subsidence in deep pillarless mining. Eng. Fail. Anal. **129**, 105631, Nov. (2021). DOI: https://doi.org/10.1016/j.engfailanal.2021.105631

[51] J. Shu, L. Jiang, P. Kong, P. Wang, P. Zhang, Numerical Modeling Approach on Mining-Induced Strata Structural Behavior by Considering the Fracture-Weakening Effect on Rock Mass. Appl. Sci. **9**, 9, 1832, May (2019). DOI: https://doi.org/10.3390/app9091832

[52] A. Darvishi, M. Ataei, R. Rafiee, Investigating the effect of simultaneous extraction of two longwall panels on a maingate gateroad stability using numerical modelling. Int. J. Rock Mech. Min. Sci. **126**, 104172, Feb. (2020). DOI: https://doi.org/10.1016/j.ijrmms.2019.104172

[53] G. Feng, P. Wang, Simulation of recovery of upper remnant coal pillar while mining the ultra-close lower panel using longwall top coal caving. Int. J. Min. Sci. Technol. **30**, 1, 55-61, Jan. (2020). DOI: https://doi.org/10.1016/j.ijmst.2019.12.017

[54] Z. Guangchao et al., Ground response of entries driven adjacent to a retreating longwall panel. Int. J. Rock Mech. Min. Sci. **138**, 104630, Feb. (2021). DOI: https://doi.org/10.1016/j.ijrmms.2021.104630

[55] G. Cheng et al., Characteristics of stratum movement induced by downward longwall mining activities in middle-distance multi-seam. Int. J. Rock Mech. Min. Sci. **136**, 104517, Dec. (2020). DOI: https://doi.org/10.1016/j.ijrmms.2020.104517

[56] P. Małkowski, Z. Niedbalski, A comprehensive geomechanical method for the assessment of rockburst hazards in underground mining. Int. J. Min. Sci. Technol. **30**, 3, 345-355, May (2020). DOI: https://doi.org/10.1016/j.ijmst.2020.04.009

[57] W. Szott, M. Słota-Valim, A. Gołąbek, K. Sowiżdżał, P. Łętkowski, Numerical studies of improved methane drainage technologies by stimulating coal seams in multi-seam mining layouts. Int. J. Rock Mech. Min. Sci. **108**, 157-168, Aug. (2018). DOI: https://doi.org/10.1016/j.ijrmms.2018.06.011

[58] E.F. Salmi, M. Karakus, M. Nazem, Assessing the effects of rock mass gradual deterioration on the long-term stability of abandoned mine workings and the mechanisms of post-mining subsidence – A case study of Castle Fields mine. Tunn. Undergr. Sp. Technol. **88**, 169-185, Jun. (2019). DOI: https://doi.org/10.1016/j.tust.2019.03.007

[59] M. Sepehri, D.B. Apel, R.A. Hall, Prediction of mining-induced surface subsidence and ground movements at a Canadian diamond mine using an elastoplastic finite element model. Int. J. Rock Mech. Min. Sci. **100**, 73-82, Dec. (2017). DOI: https://doi.org/10.1016/j.ijrmms.2017.10.006

[60] Z.P. Wu, S.H. Qiu, Y. Li, Numerical Simulation of Inclined Multi-Seam Mining Subsidence of Considered the Impact by Faults. Adv. Mater. Res. **250-253**, 2135-2140, May (2011). DOI: https://doi.org/10.4028/www.scientific.net/AMR.250-253.2135

[61] ITB. Instrukcja 416/2006. Projektowanie budynków na terenach górniczych. Warszsawa: Instytut Techniki Budowlanej, 2006.

[62] M. Kawulok, Diagnozowanie budynków zlokalizowanych na terenach górniczych. Instytut Techniki Budowlanej, 2021.

[63] K. Firek, J. Rusek, Partial least squares method in the analysis of the intensity of damage in prefabricated large-block building structures. Arch. Min. Sci. **62**, 2 (2017). DOI: https://doi.org/10.1515/amsc-2017-0020.

[64] A. Wodyński, Zużycie techniczne budynków na terenach górniczych (Technical wear of buildings in mining areas). AGH Publishing House, (2007).

[65] J. Kwiatek, Zasady oceny możliwości prowadzenia podziemnej eksploatacji górniczej z uwagi na ochronę obiektów budowlanych (ang. Principles of assessing the possibility of conducting underground mining due to the protection of buildings), Główny Inst. Górnictwa, Ser. Instr., no. 12, (2000).

[66] H. Schmidt-Schleicher, Vorschlag zur Erfassung und Bewertung historischer Bauwerke in Bergsenkungsge-bieten, Bergbau und Denkmal, 15, 77-82 (1998).

[67] V. Staege, F.W. Pohl, Ein Vorschlag zur Erfassung und Bewertung historischer Bauwerke in Bergrenkungsgebict-eneim Rahmen der Umwelt-Verträglichkertsstudie. Bauingenieur **75**, 4, 192-197 (2000).

[68] K.H. Heitfeld, M. Heitfeld, P. Rosner, H. Sahl, Kontrollierter Grubenwasseranstieg im Aachener und Sudlimburger Steinkholenrevier, in 5. Aachener Bergschandemkundliches Kolloquium, pp. 71-85, (2003).

[69] M. Heitfeld, P. Rosner, M. Mühlenkamp, H. Sahl, Bergschäden im Erkelenzer Steinkohlenrevier, in 4. Altberg-baukolloquium, pp. 281-295, (2004).

[70] E. Grun, Analyse und Prognose von Unstetigkeiten als Folge Bergbaubedinger Bodenbewegungen im linksrhei-nischen Steinkohlengebiet, Aachen RWTH. Aachen, (1995).

[71] A. Kowalski, Surface Deformation for Today's Hard Coal Mining in Poland, Górnictwo i Geoinżynieria **3**,1 (2007).

[72] T. Szwedzicki, Program for mine closure, Miner. Resour. Eng. **10**, 03, 347-364 (2001).
DOI: https://doi.org/10.1142/S0950609801000701

[73] A. Sroka, E. Grün, 2nd opinion on how mining in 479's panel in the Johann seam is likely to impact on the BAB A43 bridge over Dorstener Strasse (B225) (1996).